ADBA Chaos and Fractals
Cutting-Edge Scientific Solutions

e-ISSN: 3023-8951
RESEARCH ARTICLE
Vol.2 / No.1 / 2025 / pp.1-7
https://doi.org/10.69882/adba.chf.2025011

A Two-Memristor-based Chaotic System with Symmetric Bifurcation and Multistability

Awais Khan [*,1], **Chunbiao Li** [*,2], **Xin Zhang** [α,3] **and Xiaoliang Cen** [α,4]

*Nanjing University of Information Science & Technology, School of Artificial Intelligence, 210044, Nanjing, People's Republic of China, αNanjing University of Information Science & Technology, School of Electronic and Information Engineering, 210044, Nanjing, People's Republic of China.

ABSTRACT In this work, the study of an innovative chaotic system made from two memristors with symmetric bifurcation and multistability is presented. Within a four-dimensional chaotic framework, the system is architected with two flux-controlled memristors. Computational simulations reveal intricate dynamical phenomena such as symmetric bifurcations, multistability, and very large sensitivity to initial conditions. Using Lyapunov exponents, bifurcation diagrams, and phase portraits we investigate the system's ability to produce chaotic attractors of pronounced multistability. Pinched hysteresis loop and system offset investigation at different frequencies are investigated for possible applications in neuromorphic computing, random number generation, and secure communication protocols. We further advance our understanding of the complex dynamical properties of memristive chaotic systems. A representative analog circuit corroborates their numerical findings.

KEYWORDS
Multistability
Analog circuit
Chaotic systems
Bifurcation

INTRODUCTION

The exploitation of chaotic systems has been a main field of academic inquiry due to the many applications in secure communication, stochastic number generation, image encryption (Umar *et al.* 2024), and neuromorphic computing (Masominia 2024). In particular, memristor-based chaotic circuits (Kumari and Yadav 2023) stand out from the myriad approaches due to exceptional nonlinear properties and memristor-based memory-dependent resistance (Li *et al.* 2023). The memristor was shown to be a revolutionary element designed for nonlinear systems (Penington 2022). It is specifically well suited to chaos-oriented applications due to its ability to replicate biological synapses and exhibit intricate dynamics (Lin *et al.* 2023). Scholarly interest in memristor-based chaotic systems has been piqued for their potential applications in secure communication, random number generation, and adaptive circuits (Wei *et al.* 2024). Despite that, the existing literature is mainly about standalone memristor architectures and fails to explore the full potential of the entire set of memristors. However, two memristor-based systems remain poorly explored, in particular for their ability to increase chaos generation, symmetric bifurcation (Li *et al.* 2021), and multistability (Fang *et al.* 2022). Moreover, balanced and predictable dynamics are facilitated by symmetric bifurcation, whereas diverse and reconfigurable behaviors are supported by multistability.

The fundamental nonlinearity of the memristor brings forth a prominent characteristic of its volt-ampere characteristic curve for the memristor, which is represented by a narrowing hysteresis loop (Luo *et al.* 2023). Memristor nonlinearity embedded in the memristor fosters the development of chaotic systems exhibiting rich dynamic behaviors, such as chaos, oscillations burst multistability states, etc. (Yang *et al.* 2024). In this context, the exploration of memristive chaotic systems warrants a closer look in the field of nonlinear sciences because of the rich dynamic behaviors induced by chaotic systems realized with memristors. A considerable amount of academic research has been of interest in recent years (Lai *et al.* 2023). The controller was incorporated into the foundational memristor chaotic system to formulate a chaotic system and assess its multistability. A memristive chaotic system with remarkable multistability was introduced in the phenomenon and comprehensive studies (Bao *et al.* 2022b).

A foundational chaotic oscillating circuit incorporating a memristor that is characterized by minimal nonlinearity and bifurcation diagrams is used to explain the appearance of previously unanticipated dynamical features in the circuit (Marszalek 2022). The multiple attractors within a memristive diode bridge jerk circuit were revealed and the trajectory toward a chaotic state was investigated (Fossi *et al.* 2023). Additionally, a memristor is added to the jerk circuit and found to exhibit various dynamic attributes including multistability and monotonic behavior (Kamdem Tchiedjo *et al.* 2022).

However, a preponderance of modern academic inquiries concerns individual memristor configurations, disregarding the potential of chaotic systems consisting of dual memristors (Wang *et al.* 2024; Bao *et al.* 2022a; Guo *et al.* 2021). These rationales lead to this

Manuscript received: 21 January 2025,
Revised: 28 January 2025,
Accepted: 28 January 2025.

[1]awaiskhan3017@gmail.com (**Corresponding author**)
[2]chunbiaolee@nuist.edu.cn
[3]xinzhang96@nuist.edu.cn
[4]xiaoliangcen@nuist.edu.cn

investigation that seeks to address the gap by leveraging the interactions between a pair of memristors to enhance chaos generation, symmetric bifurcation (Guo *et al.* 2021), and multistability (Boya *et al.* 2022). In addition, further characteristics are elucidated as follows:

1. Investigate the profound multistability exhibited by a chaotic system comprising two memristors, which is contingent upon the initial conditions, through the application of a dimensionality reduction model. This methodology enables accurate forecasting examination and regulation of multistability via recognized quantitative methodologies.

2. Examine the essential dynamics, encompassing bifurcation and chaotic phenomena through the manipulation of system parameters and the subsequent observation of resultant behaviors.

3. Devise and execute an analog circuit to substantiate the theoretical conclusions, guaranteeing that the computational simulations are consistent with the empirical data.

By using the dynamics of the dimensionality reduction model to recreate the initial parameters-dependent extreme multistability in the two-memristor chaotic system, one may precisely forecast, analyze, and control extreme multistability using traditional quantitative methods.

In this article, we lay out the methodical organization of the manuscript. We focus on the evaluation of equilibrium points, Lyapunov exponents, and Kaplan-Yorke dimensions in Section 2, which describes the internal dynamics of the suggested chaotic system with two memristors. Section 3 offers an extensive exposition of the essential dynamics, encompassing chaotic attractors, bifurcation diagrams, and frequency-domain responses. Section 4 investigates the adjustable chaotic dynamics manifested by the system. Within Section 5, the occurrence of multiple attractors is scrutinized, with a specific focus on the principles of multistability and symmetric bifurcations as modulated by varied initial conditions. Section 6 articulates the conceptualization and implementation of a demonstrative analog circuit employing components such as operational amplifiers and capacitors, intended to corroborate the theoretical insights through empirical validation. The concluding section integrates the exhaustive findings and implications of the research endeavor.

MODEL AND ITS FUNDAMENTAL DYNAMICS

Chaotic Analysis of a Novel System

In this segment, we presented a novel four-dimensional framework characterized by:

$$\begin{cases} \dot{x} = -x(0.2y^2 - 0.5) - z|aw| - b \\ \dot{y} = x - 2y + 2x^2y \\ \dot{z} = x \\ \dot{w} = w - w|w| - z \end{cases} \tag{1}$$

The variables x, y, z, and w are considered independent, while the parameters a and b are positive real numbers. Altering the parameters, a and b can induce system (1) to demonstrate chaotic, periodic, or quasi-periodic behavior.

Evaluation of Equilibria

The equilibria represented by equation 1 can be determined through:

$$\begin{cases} -x(0.2y^2 - 0.5) - z|aw| - b = 0 \\ x - 2y + 2x^2y = 0 \\ x = 0 \\ w - w|w| - z = 0 \end{cases} \tag{2}$$

Equation 2 can be analyzed through analytical techniques, considering its unique equilibrium point, which is represented as S_0 $(0, 0, -0.3854, 1.2971)$. The Jacobian matrix can be formulated by linearizing Equation 1 around the zero-equilibrium point S_0:

$$J = \begin{bmatrix} 0.5 & 0 & -2.5942 & 0.7708 \\ 1 & -2 & 0 & 0 \\ 0 & 0 & 0 & 0 \\ 0 & 0 & -1 & -1.5942 \end{bmatrix} \tag{3}$$

We get the characteristic equation at S_0:

$$\det(\lambda I - J) = (a_4\lambda^4 + a_3\lambda^3 + a_2\lambda^2 + a_1\lambda^1) = 0 \tag{4}$$

Given the presence of positive Lyapunov exponents (λ_3 and λ_4), it can be inferred that the system may exhibit chaotic dynamics or unstable trajectories along certain axes. Conversely, the negative exponent (λ_1 and λ_2) implies the existence of stability along a specific direction. The system cannot be characterized as exhibiting solely stable behavior due to the presence of a positive exponent. By setting the parameters to $a = 2$ and $b = 1$, the eigenvalues relevant to the state S_0 are determined as:

$$\begin{cases} \lambda_1 = 0.3103 + 1.6628i, \\ \lambda_2 = 0.3103 - 1.6628i, \\ \lambda_3 = -1.7148, \\ \lambda_4 = -2. \end{cases} \tag{5}$$

Dimension of Kaplan-Yorke and Lyapunov Exponents

Equation 1 can be resolved utilizing the `ode45` algorithm within the MATLAB computational environment, with parameters $a = 2$ and $b = 1$ being held constant. The discretization step size is established at 0.005, which is derived from a comprehensive analysis involving one million computations. Later, with the original setup $[0.1, 0, 0, 0]$, the evaluated Lyapunov exponents were $\lambda_1 = 0.3103$, $\lambda_2 = 0.3103$, $\lambda_3 = -1.7148$, $\lambda_4 = -2$. The Kaplan-Yorke dimension of system (1) is assessed as:

$$D_{KY} = 3 + \frac{\sum_{i=1}^{3} \lambda_i}{|\lambda_4|} \tag{6}$$

$$D_{KY} = 3 + \frac{0.3103 + 0.3103 - 1.7148}{-2} = 3.5471 \tag{7}$$

The presence of an anomalous attractor is assured by the fractional quantity referred to as the Kaplan-Yorke dimension (Silva-Juárez *et al.* 2021). In Figure 1, the chaotic attractors are illustrated, while in Figure 2 it depicts the chaotic waveform, and Figure 3 represents the frequency of the chaotic signals. The signal w exhibits a reduced frequency relative to the chaotic signals.

ANALYSIS OF CHAOTIC ATTRACTORS

The chaotic attractors depicted in Figure 1 exemplify the dynamic behavior exhibited by the chaotic system based on two memristors, when the parameters $a = 2$ and $b = 1$, alongside the initial conditions $[0.1, 0, 0, 0]$. The attractors reveal intricate, non-periodic trajectories across various planes, thereby validating the chaotic characteristics of the system. Noteworthy attributes include symmetric, layered loops situated in the y-z plane, elongated and overlapping loops found in the x-z plane, and stretched intersecting loops present in the x-w plane, highlighting substantial nonlinear interactions and symmetrical bifurcation. The findings illustrate the system's ability to generate a spectrum of tunable chaotic behaviors, signifying its prospective applications in secure communication and adaptive circuitry.

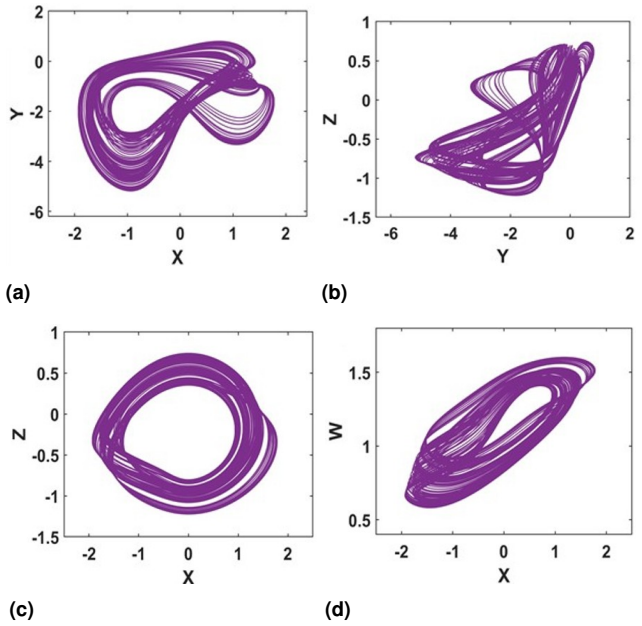

Figure 1 Chaotic attractors in different planes of equation 1 with $a = 2$ and $b = 1$ under the initial conditions $[0.1, 0, 0, 0]$: (a) x-y, (b) x-z, (c) y-z, (d) x-w.

Figure 2 delineates the erratic waveforms exhibited by the two-memristor-based chaotic system when parameters $a = 2$ and $b = 1$ are applied, under the initial conditions of $[0.1, 0, 0, 0]$. The variable outputs $x(t)$, $y(t)$, $z(t)$, and $w(t)$ exhibit irregular oscillatory patterns, which validates the chaotic features embedded within the system. Every variable displays particular amplitudes and frequencies: $x(t)$ and $w(t)$ vary within the confines of $[-2, 2]$, $y(t)$ extends from $[-6, 2]$, and $z(t)$ is bounded to $[-2, 1]$. These findings underscore the system's capacity to generate intricate, non-periodic signals that are suitable for chaos-based applications.

BIFURCATION DIAGRAMS AND LYAPUNOV EXPONENT SPECTRA

Figure 4a and 4b serve to elucidate the dynamical characteristics of the system by employing Lyapunov exponents (LEs) and bifurcation diagrams corresponding to parameter variations in a and b, respectively, under the initial conditions $[0.1, 0, 0, 0]$. When $a = 2$, the Lyapunov exponents reveal zones of chaotic dynamics, as evidenced by the positive values of the primary exponent (LE1), thereby affirming the system's pronounced sensitivity to initial

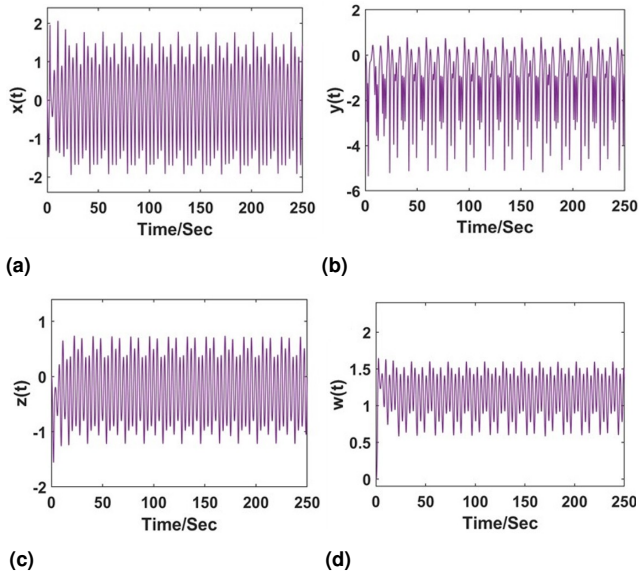

Figure 2 Chaotic Waveform of equation 1 with $a = 2$ and $b = 1$ under the initial condition $[0.1, 0, 0, 0]$: (a) waveform $x(t)$, (b) waveform $y(t)$, (c) waveform $z(t)$, (d) waveform $w(t)$.

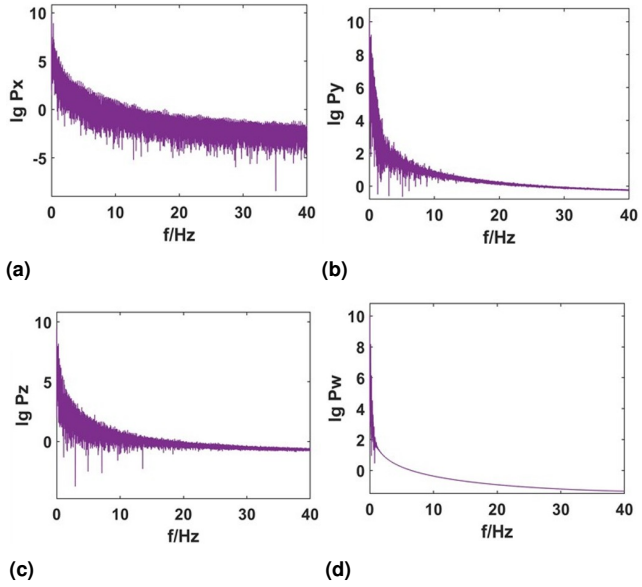

Figure 3 Frequency spectra of equation 1 with $a = 2$ and $b = 1$ under the initial conditions $[0.1, 0, 0, 0]$.

conditions. The bifurcation diagram delineates the emergence of both periodic and chaotic attractors as the parameter varies, exhibiting intricate branching patterns that encapsulate the system's dynamics. For parameter a set to 2, the Lyapunov exponents corresponding to the system (1) are represented in Fig. 4(a) as $(0.0037, -0.0469, -0.0526)$. The bifurcation diagrams of the system (1) across maximum value $[1, 2]$ at each iteration are presented in Figure 4b.

In a similar vein, when $b = 1$, the Lyapunov exponents and bifurcation diagrams unveil a comparable dynamic interplay between periodic and chaotic regimes. The positive Lyapunov exponents (LE1) corroborate the existence of chaotic domains, while the bifurcation diagram graphically represents the presence of mul-

tiple coexisting attractors and transitions between periodic and chaotic dynamics. The findings underscore the intricate dynamical behavior of the system and its adaptable characteristics through parameter variations, rendering it suitable for applications that require controllable chaos (Chaintron and Diez 2021). For a value of parameter $b = 1$, the Lyapunov exponents associated with the system (1) are $(0.0956, 0, -0.3507)$, represented in Fig. 6(a). The bifurcation diagrams of the system (1) across maximum value $[-5, 5]$ at each iteration are presented in Fig. 6b.

The preceding analysis leads to the understanding that the recommended nonlinear model can yield multiple kinds of oscillations within the nonlinear context like behaviors such as quasi-periodic, chaotic or periodic (Kuznetsov *et al.* 2023a). This significantly augmented the complexity associated with equation 1.

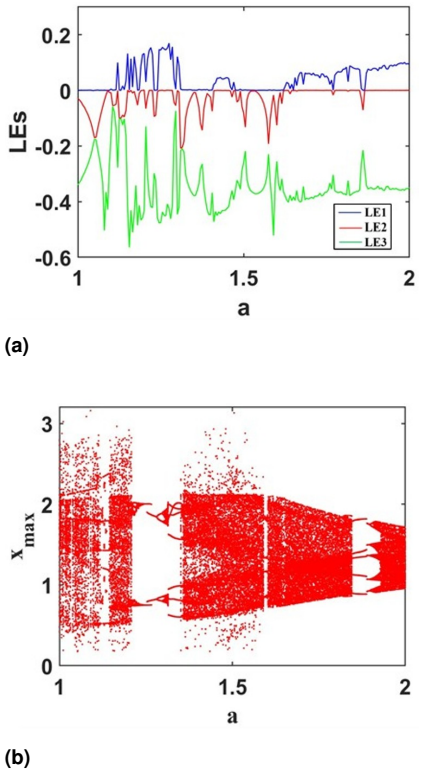

Figure 4 Dynamical behavior of equation 1 with $b = 1$ under initial conditions $[0.1, 0, 0, 0]$: (a) Lyapunov exponents, (b) bifurcation diagram.

Figure **??** illustrates the intricate dynamics of a nonlinear system as it responds to fluctuations in parameter values, specifically with b held constant at 1, while employing the initial condition of $[0.1, 0, 0, 0]$. The phase portraits delineate various modes of motion, which evolve as the parameter a is incremented. At lower values, specifically $a = 0.1$, the system demonstrates periodic behavior, typified by stable and recurrent orbits. As parameter a is increased to values such as $a = 0.8$ or $a = 2.4$, the system transitions into a regime of quasi-periodic motion, wherein the trajectories remain confined yet do not exhibit repetition. At an intermediate value of a, specifically $a = 1.6$, the system reveals chaotic dynamics, characterized by trajectories that possess multiple positive Lyapunov exponents, indicating a heightened level of complexity. For elevated values of a such as $a = 5.8$, the system manifests chaotic behavior, exhibiting sensitive dependence on initial conditions and a complex structural configuration. The parameter a governs the system's rich and multifaceted dynamics which are highlighted by these transitions among periodic, quasi-periodic, and chaotic regimes.

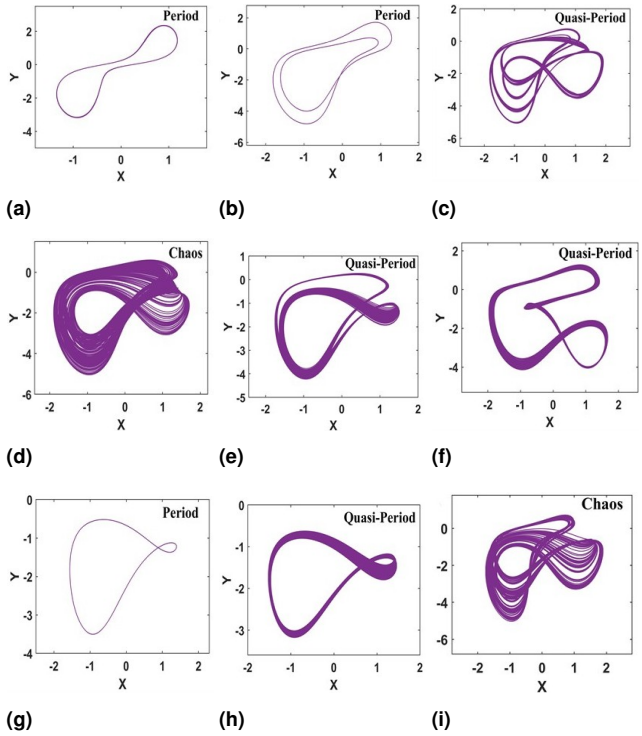

Figure 5 Typical phase portraits of equation 1 with fixed $b = 1$ under the initial condition $[0.1, 0, 0, 0]$: (a) $a = 0.1$, (b) $a = 0.8$, (c) $a = 1.6$, (d) $a = 2.1$, (e) $a = 2.4$, (f) $a = 3$, (g) $a = 4$, (h) $a = 5.5$, (i) $a = 5.8$.

Figure 7 delineates the dynamic characteristics of the nonlinear system under the constraint of a fixed parameter $a = 2$ while systematically varying the parameter b, commencing from the initial condition $[0.1, 0, 0, 0]$. When $b = 1$, the system manifests chaotic behavior, exhibiting trajectories of considerable complexity. As b is incremented to $b = 0.8$, the system transitions to quasi-periodic motion, where the trajectories remain confined yet do not exhibit repetition. At $b = 1.6$, chaotic dynamics are discerned, revealing a pronounced sensitivity to initial conditions. Ultimately, for $b = 2.1$, the system evolves into a periodic state, characterized by stable and repetitive orbits. This illustrates the system's capacity to transition among various dynamical states in response to alterations in the parameter b.

With beginning circumstances set to initial condition IC1 = $[0.1, 0, 0, 0]$ and IC2 = $[-0.1, 0, 0, 0]$, our system is shown in Figure 8 operating under the control of parameters $a = 2$ and $b = 1$. One can see the $x - w$ phase plane in Figure 8a, highlighting two unique attractors (represented in blue and red) that reflect the occurrence of periodic or quasi-periodic activity. Figure 8b outlines the temporal waveform $w(t)$, which elucidates two separate oscillatory patterns corresponding to the recognized attractors. The system exhibits intricate oscillatory behavior marked by variances in both amplitude and frequency.

MULTISTABILITY ANALYSIS

Multistability denotes the simultaneous existence of multiple trajectories under identical system parameters, characterized by distinct

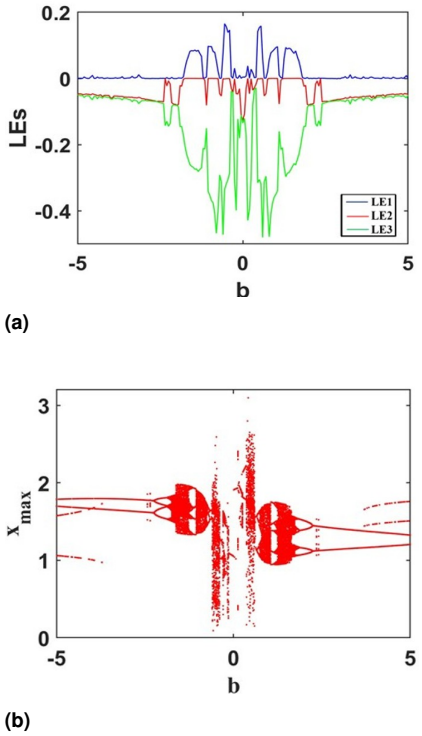

Figure 6 Dynamical behavior of equation 1 with $a = 2$ under initial conditions $[0.1, 0, 0, 0]$: (a) Lyapunov exponents of parameter b, (b) bifurcation diagram of variable x.

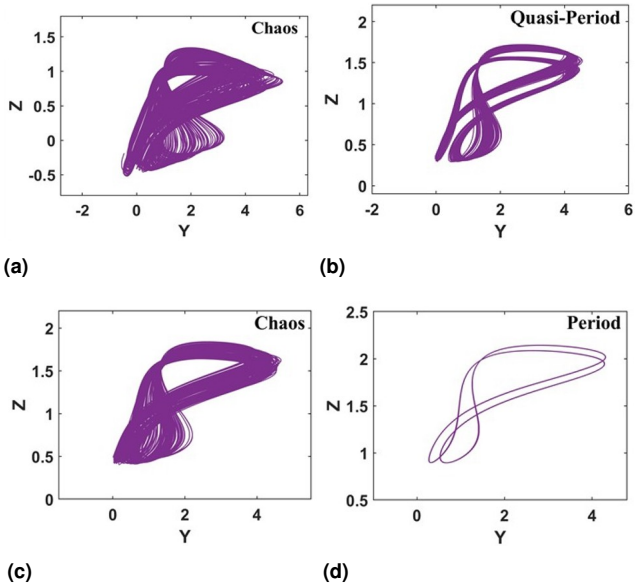

Figure 7 Typical phase portraits of equation 1 with fixed $a = 2$ under the initial condition $[0.1, 0, 0, 0]$: (a) $b = 1.5$, (b) $b = 3.6$, (c) $b = 4.1$, (d) $b = 6$.

initial conditions. Systems exhibiting multistability characteristics within chaotic dynamics are particularly advantageous for a plethora of applications in the engineering domain. This section employs Lyapunov exponents and symmetric attractors to examine the multistability intrinsic to the system under investigation. Figure 9 delineates the dynamic properties of the system for pa-

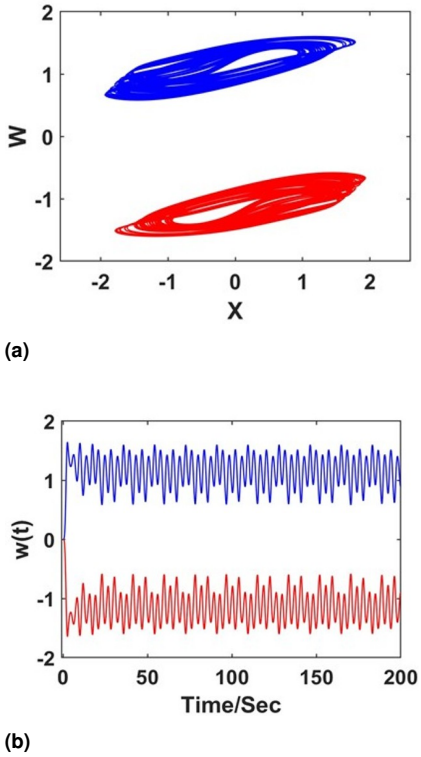

Figure 8 Coexisting symmetric chaotic attractors of equation with $a = 2$ under the initial condition IC1 = $[0.1, 0, 0, 0]$ (blue), IC2 = $[-0.1, 0, 0, 0]$ (red): (a) $x - w$ plane, (b) waveform $w(t)$.

rameter values $a = 2$ and $b = 1$, in conjunction with varying initial conditions. In Figure 9a, the observation reveals that the mean values of the system variables (x, y, z, and w) stay unchanged as $x(0)$ transitions from -5 to 5, demonstrating the equilibrium state of the system throughout this period. Figure 9b presents the Lyapunov exponents (LEs), where one exponent is marginally positive, thereby affirming the existence of chaotic dynamics, while the other exponents are negative, indicating bounded and stable trajectories within the chaotic framework.

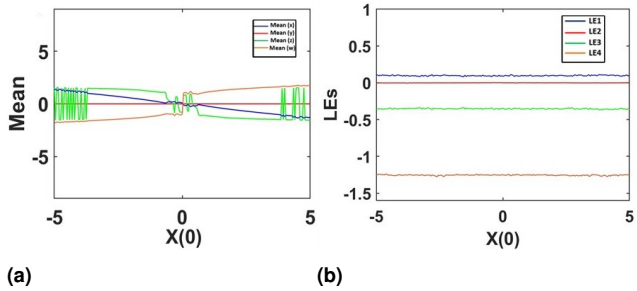

Figure 9 Dynamical behaviors of equation 1 with $a = 2$, $b = 1$ and initial conditions $[0.1, 0, 0, 0]$: (a) average values of all variables, (b) Lyapunov exponents.

The symmetric attractors showcased in Figure 10 correspond to the parameter value $a = 2$, with two mirrored initial conditions utilized, IC1 = $[0.1, 0, 0, 0]$ shown in green and IC2 = $[-0.1, 0, 0, 0]$ illustrated in red while varying the parameter b. At $b = 3.5$, symmetric chaotic attractors are evident in the system, as seen in Figure 10a. As the parameter b increases to 4.3, the attractors exhibit a

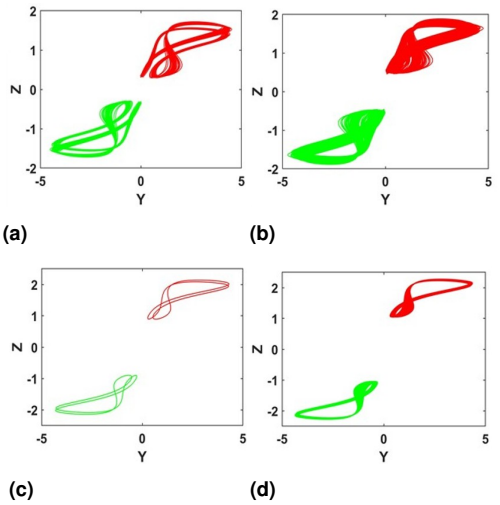

Figure 10 Coexisting symmetric attractors when $a = 2$ with initial condition IC1 = $[0.1, 0, 0, 0]$ (red), IC2 = $[-0.1, 0, 0, 0]$ (green): (a) $b = 3.5$, (b) $b = 4.3$, (c) $b = 6$, (d) $b = 6.7$.

more defined organizational structure, yet they continue to retain their chaotic characteristics as portrayed in Figure 10b. At $b = 6$, a significant transition in the system occurs, leading to periodic dynamics which is marked by the appearance of recurrent trajectories as illustrated in Figure 10c. Finally, at $b = 6.7$, the attractors attain further stabilization into symmetric periodic orbits as exhibited in Figure 10d. This figure adeptly highlights the evolution from chaotic behavior to periodic motion, concurrently sustaining symmetry as the parameter b is incrementally increased.

CIRCUIT IMPLEMENTATION

The purpose of this section is to conduct experiments in the actual world to verify theoretical results. The LM741CN operational amplifier, AD633JN multiplier, and monolithic ceramic capacitor have been employed to construct the chaotic system to validate the dynamical features of the chaotic oscillator. To facilitate meaningful comparisons, the values of the elements employed in the numerical analysis were preserved. Figure 11 illustrates the analog circuit corresponding to equation 1. The corresponding circuit state equations are articulated using Kirchhoff's law as follows:

$$\begin{cases} \dot{x} = \frac{R_{36}}{R_1 C_1}\left(\frac{-x\cdot y\cdot y}{R_{33}} + \frac{x}{R_{34}} + \frac{-z\cdot|w|}{100\cdot R_{36}} + \frac{V}{R_{37}}\right) \\ \dot{y} = \frac{R_{31}}{R_4 C_4}\left(\frac{-x}{R_{34}} + \frac{-y}{R_{23}} + \frac{x\cdot x\cdot y}{100\cdot R_{30}}\right) \\ \dot{z} = \frac{1}{R_7 C_2}x \\ \dot{w} = \frac{R_{21}}{R_{10} C_3}\left(\frac{w}{R_{18}} + \frac{-w\cdot|w|}{R_{19}} + \frac{z}{R_{20}}\right) \end{cases} \tag{8}$$

The circuit operates on a ±15V power supply. System (1) uses four state variables x, y, z, and w to describe the capacitors' state voltages across eight channels. Taking the 10kΩ resistor as a standard and setting the parameters $a = 2$ and $b = 1$, compute the appropriate parameters of the circuit elements. The parameter values are given as follows: $C_1 = C_2 = C_3 = C_4 = 1\,\text{nF}$, $R_6 = R_7 = R_9 = R_{10} = R_{11} = R_{12} = R_{13} = R_{14} = R_{15} = R_{17} = R_{18} = R_{19} = R_{20} = R_{21} = R_{22} = R_{31} = R_{32} = R_{37} = 10\,\text{k}\Omega$, $R_{23} = 5\,\text{k}\Omega$, $R_{30} = 50\,\Omega$, $R_{34} = 20\,\text{k}\Omega$, and $R_{33} = R_{35} = 500\,\text{k}\Omega$. Multisim 14.2 software was used to simulate the circuit, and Figure 12 shows the simulation outcomes. The odd attractors found

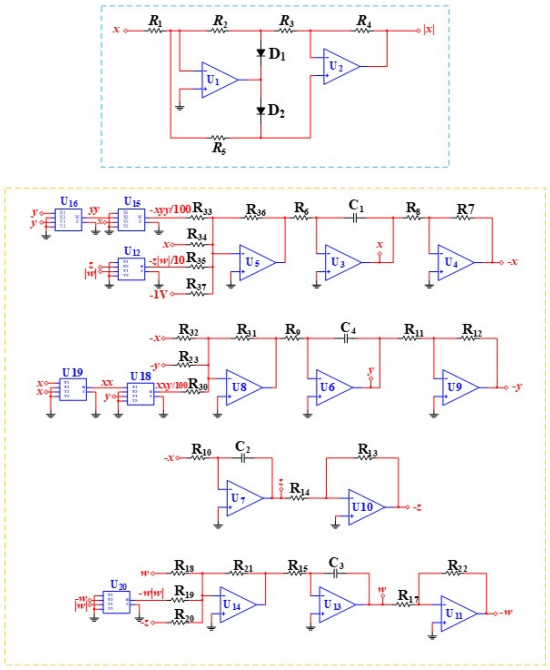

Figure 11 The chaotic oscillators modeling circuit.

in the analog circuit (Petrzela 2024) and the outcomes of the computer numerical simulation are essentially consistent (Kuznetsov *et al.* 2023b). There is some inaccuracy between the theoretical and actual findings due to the external environment and interruptions in precision.

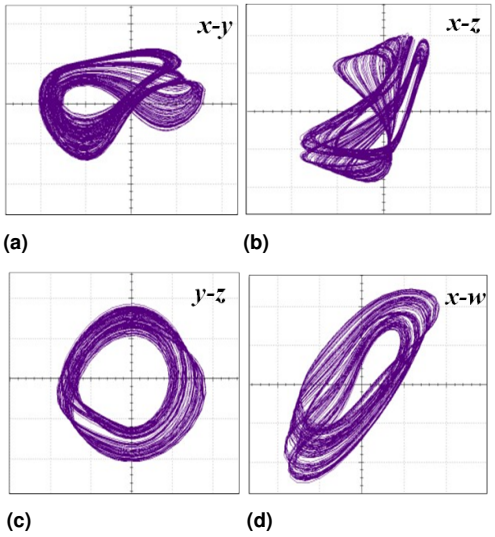

Figure 12 Circuit simulation of typical phase trajectories of equation 8 with $a = 2$, $b = 1$ under initial condition $[0.1, 0, 1, 0]$: (a) x-y plane, (b) x-z plane, (c) y-z plane, (d) x-w plane.

CONCLUSION

The investigation of the two-memristor chaotic system reveals the system's capability to generate complicated nonlinear dynamics such as symmetric bifurcation and multistability. This demonstrates that the system can be applied to secure communications,

adaptive control frameworks, and reconfigurable circuitry due to its system's intricate chaotic dynamics demonstrated by attractors, Lyapunov exponents, and bifurcation analysis. This work helps explain symmetric bifurcation and multistability by investigating the interplay of two memristors revealing how multiple attractors may exist and how chaotic behavior can be modulated. Although possessing numerous tantalizing properties, practical challenges, including experimental validation and noise robustness, as well as reconciling theoretical models with actual implementations need to be overcome to reach its full potential. This work sets the stage for further research into the design and realization of complex chaotic systems with improved functionality and robustness.

Availability of data and material

Not applicable.

Conflicts of interest

The authors declare that there is no conflict of interest regarding the publication of this paper.

Ethical standard

The authors have no relevant financial or non-financial interests to disclose.

LITERATURE CITED

Bao, H. *et al.*, 2022a Initial-condition effects on a two-memristor-based jerk system. Mathematics **10**: 411.

Bao, H. *et al.*, 2022b Parallel bi-memristor hyperchaotic map with extreme multistability. Chaos, Solitons & Fractals **160**: 112273.

Boya, B. *et al.*, 2022 The effects of symmetry breaking on the dynamics of an inertial neural system with a non-monotonic activation function: Theoretical study, asymmetric multistability, and experimental investigation. Physica A: Statistical Mechanics and its Applications **602**: 127458.

Chaintron, L.-P. and A. Diez, 2021 Propagation of chaos: a review of models, methods, and applications. ii. applications. arXiv preprint arXiv:2106.14812 .

Fang, S. *et al.*, 2022 Multistability phenomenon in signal processing, energy harvesting, composite structures, and metamaterials: A review. Mechanical Systems and Signal Processing **166**: 108419.

Fossi, J. *et al.*, 2023 Phase synchronization and coexisting attractors in a model of three different neurons coupled via hybrid synapses. Chaos, Solitons & Fractals **177**: 114202.

Guo, Q., N. Wang, and G. Zhang, 2021 A novel current-controlled memristor-based chaotic circuit. Integration **80**: 20–28.

Kamdem Tchiedjo, S. *et al.*, 2022 Dynamical behaviors of a chaotic jerk circuit based on a novel memristive diode emulator with a smooth symmetry control. The European Physical Journal Plus **137**: 940.

Kumari, U. and R. Yadav, 2023 Design and implementation of an efficient memristor-based chaotic circuit. International Journal of Information Technology **15**: 4449–4458.

Kuznetsov, A., Y. Sedova, and N. Stankevich, 2023a Coupled systems with quasi-periodic and chaotic dynamics. Chaos, Solitons & Fractals **169**: 113278.

Kuznetsov, N. *et al.*, 2023b Hidden attractors in chua circuit: mathematical theory meets physical experiments. Nonlinear Dynamics **111**: 5859–5887.

Lai, Q. *et al.*, 2023 Analysis and realization of a new memristive chaotic system with line equilibria and coexisting attractors. Journal of Vibration Engineering & Technologies **11**: 3493–3505.

Li, P. *et al.*, 2023 Dynamical properties of a meminductor chaotic system with fractal–fractional power law operator. Chaos, Solitons & Fractals **175**: 114040.

Li, P., R. Li, and C. Dai, 2021 Existence, symmetry breaking bifurcation and stability of two-dimensional optical solitons supported by fractional diffraction. Optics Express **29**: 3193–3210.

Lin, H. *et al.*, 2023 Memristor-coupled asymmetric neural networks: Bionic modeling, chaotic dynamics analysis and encryption application. Chaos, Solitons & Fractals **166**: 112905.

Luo, N. *et al.*, 2023 Well-defined double hysteresis loop in nanbo3 antiferroelectrics. Nature Communications **14**: 1776.

Marszalek, W., 2022 On physically unacceptable numerical solutions yielding strong chaotic signals. Entropy **24**: 769.

Masominia, A., 2024 *Neuro-inspired computing with excitable micro-lasers*. Ph.D. thesis, Université Paris-Saclay.

Penington, T., 2022 *A non-linear model and framework for implementing transformative change*. Ph.D. thesis, Victoria University.

Petrzela, J., 2024 Chaotic systems based on higher-order oscillatory equations. Scientific Reports **14**: 21075.

Silva-Juárez, A. *et al.*, 2021 Optimization of the kaplan-yorke dimension in fractional-order chaotic oscillators by metaheuristics. Applied Mathematics and Computation **394**: 125831.

Umar, T., M. Nadeem, and F. Anwer, 2024 Chaos-based image encryption scheme to secure sensitive multimedia content in cloud storage. Expert Systems with Applications **257**: 125050.

Wang, Q. *et al.*, 2024 A novel 4d chaotic system coupling with dual-memristors and application in image encryption. Scientific Reports **14**: 29615.

Wei, X. *et al.*, 2024 Nonlinear analysis, circuit design, and chaos optimization application of multiscroll chaotic attractors based on novel locally active non-polynomial memristor. Nonlinear Dynamics pp. 1–38.

Yang, F., J. Ma, and F. Wu, 2024 Review on memristor application in neural circuit and network. Chaos, Solitons & Fractals **187**: 115361.

How to cite this article: Khan, A., Li, C., Zhang, X., and Cen, X. A Two-memristor-based Chaotic System with Symmetric Bifurcation and Multistability. *Chaos and Fractals*, 2(1), 1-7, 2025.